Pure nuclear Bragg reflection of a periodic $^{56}Fe/^{57}Fe$ multilayer

L. Deák[a)]
KFKI Research Institute for Particle and Nuclear Physics, P.O.B. 49, H-1525 Budapest, Hungary

G. Bayreuther
Institut für Angewandte Physik, Universität Regensburg, Universitätsstr. 31, D-93053 Regensburg, Germany

L. Bottyán
KFKI Research Institute for Particle and Nuclear Physics, P.O.B. 49, H-1525 Budapest, Hungary

E. Gerdau
II. Institut für Experimentalphysik, Universität Hamburg, Luruper Chaussee 149, D-22761 Hamburg, Germany

J. Korecki
Department of Solid State Physics, University of Mining & Metallurgy, al. Mickiewicza 30, PL-30-059 Kraków, Poland

E. I. Kornilov
Frank Laboratory of Neutron Physics, Joint Institute for Nuclear Research, 141 980 Dubna, Moscow Region, Russia

H. J. Lauter
Institute Laue-Langevin, B.P. 156, F-38042 Grenoble Cedex 9, France

O. Leupold
II. Institut für Experimentalphysik, Universität Hamburg, Luruper Chaussee 149, D-22761 Hamburg, Germany

D. L. Nagy
KFKI Research Institute for Particle and Nuclear Physics, P.O.B. 49, H-1525 Budapest, Hungary

A. V. Petrenko and V. V. Pasyuk-Lauter[b)]
Frank Laboratory of Neutron Physics, Joint Institute for Nuclear Research, 141 980 Dubna, Moscow Region, Russia

H. Reuther and E. Richter
Forschungszentrum Rossendorf e.V., Institut für Ionenstrahlphysik und Materialforschung, Pf. 510119, D-01314 Dresden, Germany

R. Röhloberger[c)]
II. Institut für Experimentalphysik, Universität Hamburg, Luruper Chaussee 149, D-22761 Hamburg, Germany

E. Szilágyi
KFKI Research Institute for Particle and Nuclear Physics, P.O.B. 49, H-1525 Budapest, Hungary

(Received 3 March 1998; accepted for publication 3 October 1998)

Grazing incidence nuclear multilayer diffraction of synchrotron radiation from a periodic stack of alternating ^{56}Fe and ^{57}Fe layers was observed. Resonant layer fraction, substrate size, flatness, and surface roughness limits were optimized by previous simulations. The isotopic multilayer (ML) sample of float glass/^{57}Fe(2.25 nm)/[^{56}Fe(2.25 nm)/^{57}Fe(2.25 nm)]×15/Al(9.0 nm) nominal composition was prepared by molecular beam epitaxy at room temperature. Purity structure and lateral homogenity of the isotopic ML film was characterized by magnetometry, Auger electron, Rutherford backscattering, and conversion electron Mössbauer spectroscopies. The isotopic ML structure was investigated by neutron and synchrotron Mössbauer reflectometry. Surface roughness of about 1 nm of the flat substrate (curvature radius >57 m) was measured by scanning tunneling microscopy and profilometry. A pure nuclear Bragg peak appeared in synchrotron Mössbauer reflectometry at the angle expected from neutron reflectometry while no electronic Bragg peak was found at the same position by x-ray reflectometry. The measured width of the Bragg peak is in accordance with theoretical expectations. © *1999 American Institute of Physics.* [S0021-8979(99)09201-4]

[a)]Electronic mail: deak@rmki.kfki.hu
[b)]Present address: Universität Konstanz, Postfach 5560, D-78434 Konstanz, Germany.
[c)]Present address: Universität Rostock, August-Bebel-Str. 55, D-18055 Rostock, Germany.

I. INTRODUCTION

In nuclear resonant scattering (NRS) of synchrotron radiation (SR) low-lying levels of an ensemble of identical nuclei are coherently excited by the synchrotron radiation pulse. Since the levels are, as a rule, split by hyperfine interactions, the spatial and temporal coherence of the scattering results in characteristic patterns both of the angular distribution and the time evolution of the scattered radiation, which bear simultaneous and correlated information about topology and internal fields in the sample under study. SR is scattered both by nuclei and by electrons and these two processes interfere with each other, as well.

Conventional Mössbauer spectroscopy and NRS of SR are, although delivering similar information on hyperfine interaction and lattice dynamics, complementary rather than equivalent to each other. The principal difference is that when the energy spectrum is scanned by the Doppler-shifted radiation of a γ source, the recorded signal presents the incoherent sum of the spectral components of the transmitted radiation. In case of time domain NRS of SR, however, the response is formed by the coherent sum of the spectral components of the scattered radiation. From practical points of view however, NRS of SR has various advantages. Due to the high brilliance, the low divergence, the high degree of polarization and the pulsed time structure of SR, Mössbauer-like measurements on extremely small samples have become possible. Further, the performance of grazing incidence NRS experiments can be improved by several orders of magnitude by using SR rather than radioactive sources, a fact opening the way to a new kind of depth selective hyperfine spectroscopy, viz. synchrotron Mössbauer reflectometry (SMR).[1–4]

NRS experiments at synchrotron beamlines are now routinely performed in (a) forward scattering, (b) grazing incidence, and (c) Bragg reflection geometries. The high count rate of the direct beam and of the prompt electronic scattering poses major detector dead time problems in forward scattering experiments. SMR is usually performed close to or even below the critical angle of the electronic total reflection where, due to the interplay of electronic and nuclear scattering, a considerable amount of delayed photons along with a high intensity of electronically reflected prompt photons are available.[3,5] Nuclear Bragg reflections may also electronically be allowed, a fact leading to the same detection problem. One of the keys to high performance NRS experiments with SR is the development of monochromators with an energy bandpass in the order of the hyperfine interaction energy (i.e., $\approx$1 μeV). A narrower bandwidth leads to a partial excitation of the hyperfine levels of the probe nuclei and a response time comparable to the nuclear lifetime while a broader one unnecessarily overloads the detector with nonresonant radiation.

The angular acceptance of the monochromator should not be less than the divergence of the synchrotron radiation beam typically of 20–60 μrad at bending magnets and undulators and several hundreds of μrad at wigglers. The bandwidth of $\approx$1 μeV can be achieved by use of a pure nuclear Bragg reflection of a single crystal due to the hyperfine interaction of the nuclei delivering a rather complicated energy spectrum. The angular acceptance of a single crystal nuclear Bragg monochromator is $\sim$20 μrad. Nonresonant nested channel-cut monochromators have the suitable angular acceptance their energy bandwidth being, however, $\gtrsim$1 meV. Two kinds of nuclear monochromators of suitable bandwidth *and* angular acceptance have been suggested so far, viz. grazing incidence antireflection (GIAR) films[6,7] and synthetic periodic multilayers. Synthetic periodic multilayers should have a nuclear Bragg reflection at a glancing angle Θ which is well above the critical angle of the electronic total reflection so that the electronic reflectivity of the mirror at Θ is low enough. Both kinds of narrow band monochromators have roughly the same bandpass and reflectivity irrespective of the particular multilayer design, so that the real differences in existing multilayer devices are of technical nature.

The fabrication both of GIAR films and of synthetic periodic multilayers is difficult due to various technological problems. The substrate should be extremely flat and the roughness of the surface as well as of the interfaces should be suppressed, the same holding true for a possible interdiffusion of the layers. Also a sufficient lateral homogeneity of the mirrors should be ensured. In what follows we shall restrict ourselves to the 14.413 keV resonance of ^{57}Fe.

Pure nuclear reflections are expected from two kinds of synthetic periodic multilayers. In the first group the hyperfine interaction in different layers has a superstructure as compared to the interlayer spacing. The second group comprises synthetic periodic multilayers built from alternating resonant and nonresonant isotopes of the same element (synthetic isotopically periodic multilayers). Typical examples of the first class are antiferromagnetically coupled multilayers. Pure nuclear reflections of SR from an Fe/Cr multilayer with a Cr thickness of 1.0 nm mediating an antiferromagnetic interaction between the Fe layers have been observed by Toellner *et al.*[8] Recently, pure nuclear reflections of antiferromagnetic origin have been observed on Fe/FeSi multilayers.[9]

The idea of building nuclear monochromators from synthetic isotopically periodic multilayers was first suggested by Trammell *et al.*[10] and also discussed later by Kabannik.[11] In a short communication,[12] Kikuta *et al.* reported on the fact of having observed the pure nuclear reflection of the 14.413 keV radiation of a ^{57}Co source from a $[^{56}\mathrm{Fe}(1.2\ \mathrm{nm})/^{57}\mathrm{Fe}(0.8\ \mathrm{nm})]\times n$ synthetic isotopically periodic multilayer. Unfortunately, very few details of sample preparation and measurement are given. The systematic design and development of synthetic isotopically periodic multilayer monochromators started in 1991 when Chumakov and Smirnov[13] optimized the total thickness t and bilayer thickness d as well as the ratio β of the thickness of the resonant layer to d. Since then, there have been various attempts (*vide infra*) to prepare synthetic isotopically periodic multilayers with the sputtering technique and to observe their pure nuclear reflections.

The fabrication of ^{56}Fe/^{57}Fe multilayers with sputtering had failed[14] due to interdiffusion of ^{56}Fe and ^{57}Fe into each other. Conversion electron Mössbauer spectra (CEMS) of such samples showed α-iron, with some asymmetric broadening of the lines towards lower magnetic fields.[14]

Chumakov *et al.*[15] reported the observation of the nuclear reflection of 14.413 keV radiation from a ^{57}Co source, using a synthetic periodic multilayer $[^{57}\mathrm{Fe}(2.0\ \mathrm{nm})/\mathrm{Sc}(3.3\ \mathrm{nm})]\times 20$ on an extremely smooth glass substrate. Due to the lack of isotopic periodicity of iron, the reflection was also electronically allowed. The iron layers were amorphous and nonmagnetic. Later, a pure nuclear reflection of the ^{57}Co gamma radiation was observed[16] using a synthetic isotopically periodic multilayer $[^{57}\mathrm{Fe}(2.2\ \mathrm{nm})/\mathrm{Sc}(1.1\ \mathrm{nm})/\mathrm{Fe}(2.2\ \mathrm{nm})/\mathrm{Sc}(1.1\ \mathrm{nm})]\times 25$. Clearly, the electronic Bragg peak of this mirror lies at double the angle of the pure nuclear reflection. The first attempt to see the pure nuclear reflection of synchrotron radiation from a synthetic isotopically periodic multilayer was made by Chumakov *et al.*,[17] using this [^{57}Fe/Sc/Fe/Sc] mirror. In this experiment the nuclear Bragg peak was seen, and the applicability of the mirror as a nuclear monochromator was demonstrated. Nevertheless, as seen in Fig. 1 of the corresponding paper,[17] a weak electronic Bragg peak of reflectivity at the 10^{-3} level also appeared together with the nuclear one. The first demonstration of a pure nuclear reflection from a synthetic isotopically periodic multilayer having no electronic Bragg peak at all was by Röhlsberger *et al.*,[18] using a ^{57}Co source and a multilayer $[^{56}\mathrm{Fe_5B_4C}(4.8\ \mathrm{nm})/^{57}\mathrm{Fe_5B_4C}(3.9\ \mathrm{nm})]\times 10$.

In an attempt to test the capabilities of molecular beam epitaxy (MBE) in fabricating μeV monochromators for nuclear resonant scattering experiments at synchrotrons, we prepared a synthetic isotopically periodic multilayer from alternating layers of ^{56}Fe and ^{57}Fe. After extensive characterization of the sample with various methods we found a pure nuclear reflection of SR.

II. EXPERIMENT

A. Sample design

When designing the nuclear resonant mirror we focussed on three items: (a) to optimize the structure of the multilayer so that the reflectivity of the monochromator at the nuclear Bragg peak should be maximum (b) to select a flat substrate of low surface roughness, and (c) to choose a preparation method by which interdiffusion, enhanced interface roughness, and amorphization can be avoided and a sufficient lateral homogeneity can be ensured.

The bilayer thickness d of the multilayer was selected following the criteria of Chumakov and Smirnov[13] viz. by prescribing a low ($10^{-2}\cdots 10^{-3}$) electronic reflectivity at the expected Bragg angle. The nominal bilayer thickness d was chosen to be 4.5 nm corresponding to a Bragg angle $\Theta_B=\sqrt{(\lambda/2d)^2+\Theta_c^2}=10.3$ mrad with $\lambda=0.0860$ nm of the 14.413 keV radiation and $\Theta_c=3.8$ mrad (the critical angle of electronic total reflection of α-iron for this wavelength). At $\Theta=10.3$ mrad the electronic reflectivity of a semi-infinite α-iron has been calculated[13] with the Fresnel formula to be $\approx 10^{-3}$.

The ratio β of the thickness of the resonant layer to d was optimized utilizing the technique of characteristic matrices;[19] more details of the numerical technique were given elsewhere.[2,3] Our optimization criterium was slightly different from that of Chumakov and Smirnov.[13] While these authors optimized the reflectivity $R(E,\Theta)=|r(E,\Theta)|^2$ as averaged around the resonant energy E_0 over an energy interval of ≈ 1 μeV at the Bragg angle Θ_B (and neglected the electronic scattering) we suggested that, for time domain experiments, it was more reasonable to optimize the integral.

$$D(\Theta_B)=\int_{\Theta_B-\Delta\Theta/2}^{\Theta_B+\Delta\Theta/2}\int_{t_1}^{t_2}R_t(t,\Theta)\,dt\;d\Theta,$$

with $R_t(t,\Theta)=|r_t(t,\Theta)|^2$ where r_t is the time domain reflectivity amplitude, the Fourier transform of the energy domain reflectivity amplitude $r(E,\Theta)$, $\Delta\Theta$ is the divergence of the synchrotron radiation, while t_1 and t_2 are the limits of the time window set to detect the delayed photons. With $t_1=12$ ns, $t_2=175$ ns, and $\Delta\Theta=50$ μrad (and accounting for nuclear *and* electronic scattering) $D(\Theta_B)$ was found to be maximum for $\beta=0.4\cdots 0.5$ depending on the number of bilayers, i.e., at values somewhat higher than $\beta=0.33$ as calculated by Chumakov and Smirnov.[13]

The proper selection of the material and of the dimensions of the substrate is a crucial problem. A surface and interface roughness of $R_q\gtrsim 1.5$ nm will considerably attenuate or even completely smear out both the structural Bragg peak and the Kiessig oscillations related to the total thickness of the multilayer. Clearly, the surface roughness of the substrate should by no means exceed this value. Commercial Si wafers and cleaved single crystals often have $R_q>1.5$ nm. Therefore we decided to use a high quality float glass substrate with a nominal $R_q=0.5$ nm. The optimum length l of the substrate is given by $l=\Delta z/\Theta_B$ where Δz is the height of the synchrotron beam (≈ 1 mm at beamline F4 of HASYLAB) in order not to lose intensity due to grazing incidence geometry. Unfortunately, as we shall see, the resulting $l\approx 10$ cm cannot easily be realized and a considerable loss in intensity should be accepted.

The flatness (i.e., the long scale curvature radius ρ_c) of the sample is given by the condition that the angle of the substrate plane normal between two opposite ends of the sample should be less than or approximately equal to an acceptable fraction κ (say 20%) of the expected width of the Bragg peak $\Delta\Theta_B$, in other words $\rho_c\gtrsim l/\kappa\Delta\Theta_B$. Taking $l\approx 10$ cm, $\Delta\Theta_B=1$ mrad, and $\kappa=0.2$, we have $\rho_c\gtrsim 500$ m, a condition not easy to fulfill. For a substrate of a given curvature ρ_c the condition for the length $l\lesssim\rho_c\kappa\Delta\Theta_B$ can be used.

Another and opposite limit for l is given by the preparation conditions in view of the demand of a sufficient lateral homogeneity of the layer thickness (*vide infra*) and by other technical limitations of a given evaporation chamber. Besides, the substrate should be thick enough in order to prevent the sample from bending. With all these in mind, the dimensions of the float glass substrate were selected to be 15 mm$\times$15 mm$\times$1 mm. With $l=15$ mm, the condition for the curvature $\rho_c\gtrsim 75$ m was set.

In order to avoid interdiffusion of the two iron isotopes during preparation we decided to use a preparation technique by which the energy of the deposited atoms can be well controlled and also a proper crystallinity of the layers is expected. In view of the difficulties in previous attempts to

prepare synthetic isotopically periodic multilayers by sputtering or by conventional vacuum evaporation techniques, we decided to use the MBE technique. One of the basic problems of MBE is to optimize the distance h of the substrate from the evaporation cells. On one hand, if h is too high, the deposition yield of the expensive isotope ^{57}Fe will be low; on the other hand, if h is too low, the lateral homogeneity of the layer thickness will suffer. We note that, as a rule, it is quite difficult to ensure a controlled ^{57}Fe deposition yield with magnetron sputtering. Clearly, the relative lateral layer thickness inhomogeneity should be less than or about $\kappa\Delta\Theta_B/\Theta_B$ ($\lesssim$2% with the above values) otherwise the Bragg peak will be smeared out. Simple geometrical consideration sets the condition $l/h \lesssim 2\sqrt{\kappa\Delta\Theta_B/\Theta_B}$, provided that $\kappa\Delta\Theta_B/\Theta_B \ll 1$. With the above values we have $h \gtrsim 5.4$ cm.

B. Sample preparation and characterization

The synthetic isotopically periodic multilayer sample of nominal structure float glass/^{57}Fe(2.25 nm)/[^{56}Fe(2.25 nm)/^{57}Fe(2.25 nm)]$\times$15/Al(9.0 nm) (sample ''^{56}Fe/^{57}Fe multilayer,'' for later use) was grown with MBE in a ultrahigh vacuum (UHV) deposition chamber built at the University of Mining & Metallurgy, Kraków, Poland. The distance between the evaporation cells and the substrate was $h=7$ cm. The base pressure during evaporation was better than 10^{-8} Pa, the deposition rate was 0.8 nm/s. The BeO crucibles of the Knudsen cell contained ^{57}Fe (of 95% enrichment) and ^{56}Fe. During deposition, the float glass substrate was held at room temperature. The substrate was heated prior to preparation to about 150 °C. The evaporation rate was monitored with a quartz gauge with an accuracy corresponding to 0.01 nm. The average thickness of a single isotope Fe layer was kept within an accuracy better than $\pm$0.1 nm as compared with the nominal one. The Fe layer structure was coated with Al in order to prevent the iron film from oxidizing. As we shall see, the Al coating turned out to be inhomogeneous. This fact, however, had no serious influence on the reflectivity of the sample.

The flatness of the sample was determined by a Dektak 8000 surface profilometer. The long scale curvature radius ρ_c turned out to be not less than 57 m, roughly fulfilling the requirement $\rho_c \gtrsim 75$ m.

Both *in situ* and conventional CEMS showed the presence of pure α-iron. The resonance lines, as shown in Fig. 1, had no significant broadening, their relative intensities being 2.80:3.42:1.00, i.e., close to 3:4:1 characteristic for the magnetization lying in the sample plane. The hyperfine field [$H_{\rm hf}$=33.0(1) T] corresponds to that of α-Fe within the experimental error. Vibrating sample magnetometry also supported the presence of α-iron with a coercivity field of 30 Oe at room temperature.

Sputter depth profiling was performed with a scanning Auger electron spectrometer MICROLAB 310F. The relatively low value of ρ_c and d prevented us from exactly measuring the depth of the sputtering crater with the profilometer. Nevertheless, the obtained depth (about 60 nm) was still in fair accordance with the nominal value of 72.8 nm. Sputtering was performed on the rotating sample with a 3 keV

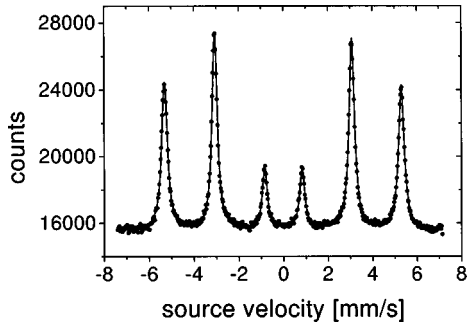

FIG. 1. Conversion electron Mössbauer spectrum of the ^{56}Fe/^{57}Fe multilayer at room temperature taken in a flow of 96 vol. % He and 4 vol. % CH_4 counter gas with a ^{57}Co(RH) source. Velocity scale is given relative to α-Fe at room temperature.

Ar^+ ion beam at a current density of about 0.5 mA/mm^2. The Auger peaks Fe(LMM) at 703 eV, O(KLL) at 507 eV, and C(KLL) at 266 eV were used for the analysis. The observed profiles (see Fig. 2) indicated no oxidization in the majority of the iron layers. Carbon appeared only in the uppermost 1 nm of the multilayer and the uppermost 5 nm turned out to be oxidized. Another 5$\cdots$10 nm of iron at the Fe/glass interface seemed to be oxidized, as well. No significant Auger peak of Al could be identified. We explain this fact by the already mentioned inhomogeneity (a strong wedge-like shape) of the Al coating thickness. Indeed, in order not to damage the mirror, Auger profiling was done close to one corner of the sample.

The short scale surface roughness of the sample was measured by scanning tunnel microscopy on a Rasterscope 3000 instrument. Long scale surface roughness data were also extracted from surface profilometry. Both methods resulted in roughness values of $R_q \approx 1$ nm.

The total amount of iron at different beam spots was determined by Rutherford backscattering spectrometry (RBS) using a 1.62 MeV $^4He^+$ beam obtained from a 5 MeV Van de Graaff accelerator of the KFKI Research Institute for Particle and Nuclear Physics, Budapest. An ion current of typically 20 nA as measured by a transmission Faraday cup[20] was used. Figure 3 shows the measured RBS spectrum taken at the spot closest to the center of the sample (''central spec-

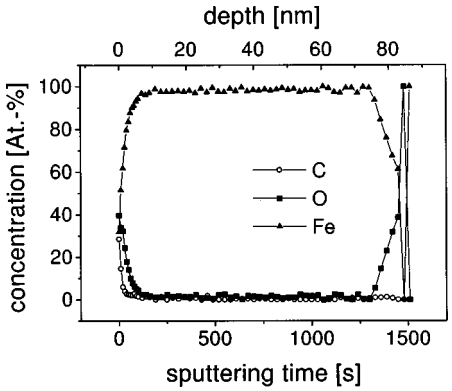

FIG. 2. Sputtering Auger electron spectroscopy depth profile of the ^{56}Fe/^{57}Fe multilayer. The calibration of the depth scale was determined by the total iron thickness of 82.6 nm as taken from neutron reflectometry data.

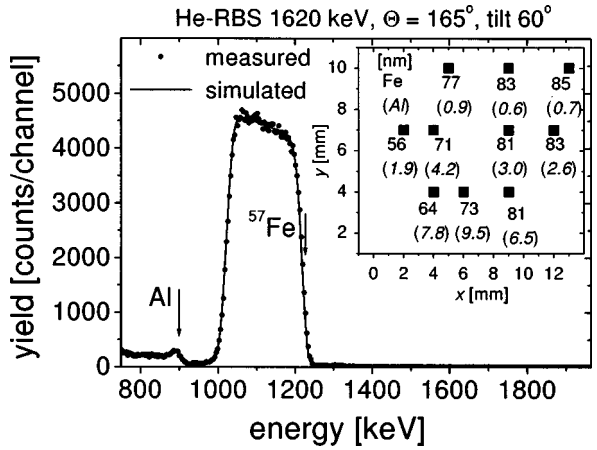

FIG. 3. RBS spectrum taken close to the center (x=8.5 mm, y=7.0 mm) of the ^{56}Fe/ ^{57}Fe multilayer using a 50 mm^2 ORTEC surface barrier detector at 165° scattering angle with a solid angle of 5.5 msr. The sample was tilted at 60°. The arrows show the energy belonging to the respective elements on the surface. The inset displays the Fe and Al thicknesses at ten different spots (normal and *italic* numbers, repsectively).

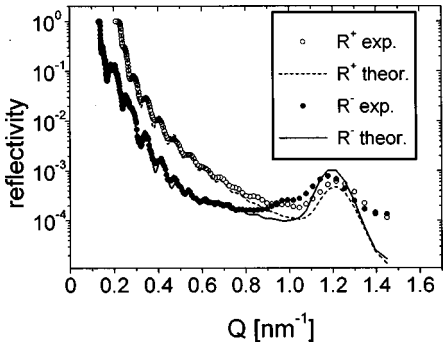

FIG. 4. Measured spin dependent neutron reflectivities R^+ and R^- of the ^{56}Fe/ ^{57}Fe multilayer as a function of the momentum transfer Q. The fit curves correspond to the float glass/^{57}Fe(4.6 nm)/[^{56}Fe(2.9 nm)/ ^{57}Fe(2.3 nm)]×15/Al(5.7 nm) structure.

trum'') as well as the simulated one determined by the RBX program[21] using a layer structure of float glass/Fe(81 nm)/Al(3 nm). The peak areas of Fe and Al as a function of beam position were used to create a ''homogeneity map'' of the sample (inset in Fig. 3). Normalization was performed to the respective peak areas of the central spectrum. Unfortunately, the expectation for the lateral homogeneity of the iron thickness to be $\lesssim$2% has not been fulfilled, its overall value being $\approx$15%. Nevertheless, about one half of the sample ($x>8$ mm; see inset) turned out to be good enough for the synchrotron measurements.

C. Polarized neutron reflectometry

The only established method capable of testing the quality of synthetic isotopically periodic multilayers is neutron reflectometry. In fact, in contrast to x rays, the nuclear scattering length of neutrons is different for different isotopes of the same chemical element. Therefore, a structural Bragg peak at about the same values of the scattering vector (momentum transfer) Q should appear from synthetic isotopically periodic multilayers in neutron reflectometry and in SMR experiments while no such peak is expected in nonresonant x-ray reflectometry due to the homogeneous electronic density of the sample. Furthermore, neutron reflectometry with polarized neutrons is capable of revealing the magnetic structure of the film.

The objective of the polarized neutron reflectometry experiment is to obtain the reflectivities R^+ and R^- for up and down spin neutrons (with respect to the applied magnetic field) as a function of Q. The measured reflectivities $R^{\pm}(Q)$ are functionals of the nuclear and magnetic neutron scattering length profiles $b_n(z)$ and $b_m(z)$, respectively, along the depth z, so that $R^{\pm}(Q)=F[(b_n(z)/V \pm b_m(z)/V)]$ with $b_m(z)=C\mu(z)$, where $Q=4\pi \sin\Theta/\lambda$ and $C=r_0\gamma/2 = 0.269\,542\times10^{-12}$ cm/μ_B [where λ is the neutron wavelength, r_0 is the classical electron radius, γ=1.91304 is the magnetic moment of the neutron in nuclear magnetons, V is the atomic volume and, $\mu(z)$ is the average magnetic moment per atom at depth z]. For ferromagnetic films magnetized in the sample plane no spin-flip processes take place and the functional F can easily be calculated using the technique of characteristic matrices.[19,22]

The neutron reflectometry measurements of the ^{56}Fe/^{57}Fe multilayer were made at the time-of-flight polarized neutron spectrometer (SPN) at the pulsed reactor IBR-2 at the Joint Institute for Nuclear Research at Dubna.[23] The neutron wavelength ranged from 0.08 to 0.12 nm. Experimental spin-dependent reflectivities R^+ and R^- were obtained by applying the saturating external magnetic field of 0.1 T parallel to the film surface and are shown together with the fit to the data in Fig. 4. The oscillations correspond to a total thickness of the sample of 88.3 nm. A Bragg peak appears around the momentum transfer value $Q=1.2$ nm^{-1} both on the R^+ and R^- reflectivity curves. The Bragg peak position is determined by the thickness of the isotope bilayer structure. To establish the scattering length density in the float glass a reflectivity curve of substrate was measured separately. The degree of polarization of the neutrons has been independently measured and has properly been accounted for. From the fit to the data we determined the structure and the interfacial roughness of the film. The layer structure was fitted to be float glass/^{57}Fe(4.6 nm)/[^{56}Fe(2.9 nm)/^{57}Fe(2.3 nm)] ×15/Al(5.7 nm) along with the roughness values R_q of 2.0, 1.0, and 1.8 nm on the surface, at the interfaces and on the substrate, respectively. The thickness higher than nominal of the ^{57}Fe layer near substrate is probably due to the presence of oxygen and to a small diffusion of Fe into the glass.

D. Synchrotron Mössbauer reflectometry

SMR experiments were performed at the nuclear resonance scattering beamline F4 of HASYLAB, DESY, Hamburg. The 14.413 keV resonant radiation was selected with a Si(111) high heat load monochromator and a Si(4 2 2)/Si(12 2 2) nested channel-cut monochromator. The height of the synchrotron radiation beam was adjusted to 60 μm, the vertical divergence was about 20 μrad. The beam width was adjusted between 1 and 4 mm according to the experimental requirements (*vide infra*).

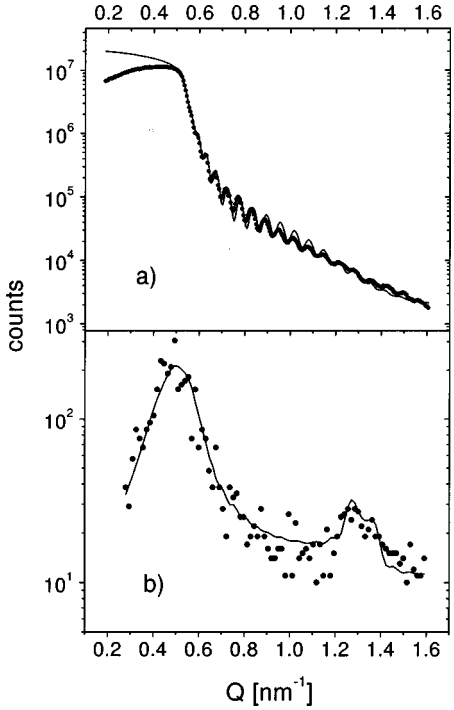

FIG. 5. Nonresonant x-ray curve (a) and time integral delayed (resonant) reflectivity (b) of SR from the ^{56}Fe/ ^{57}Fe multilayer. Delayed counts were collected in the time interval $17\ \text{ns} < t < 146\ \text{ns}$ at glancing angle corresponding to momentum transfer Q. The continuous curves were calculated from the layer parameters of the neutron reflectivity fit for the float glass/ ^{57}Fe(4.6 nm)/[^{56}Fe(2.9 nm)/^{57}Fe(2.3 nm)]×15/Al(5.7 nm) structure.

In view of the lateral homogeneity data, as inferred from the RBS measurements, the most homogeneous part of the sample had to be selected. First the multilayer was oriented with the y axis (Fig. 3) parallel to the beam. This direction enables one to illuminate the largest possible homogeneous part of the sample. Afterwards, the most homogeneous part of the sample ($x > 8$ mm) was selected by subsequent x-ray reflectometry measurements performed at parallel strips of the sample with a beam of 1 mm width. It was established that the region is homogeneous enough to observe the Bragg peak. Then nuclear resonant scattering experiment was done only on this part of the sample with a beam width of 4.0 mm. For technical reasons, it was not possible to apply an external magnetic field. A series of time integral rocking curves was recorded and added ($t_1 = 17$ ns, $t_2 = 131$ ns). The sum of the measurements taken in a run of about 10 h is shown in Fig. 5. The first peak at $Q = 0.56\ \text{nm}^{-1}$ is due to the interplay of the electronic and nuclear scattering at the critical angle of the electronic total reflection.[3,5] The second one is the Bragg peak that was found on the resonant reflectivity curve almost exactly at the same value of the momentum transfer ($Q = 1.25\ \text{nm}^{-1}$) as in the neutron experiment. At the same time, no Bragg peak can be seen on the nonresonant x-ray reflectivity curve (Fig. 5). Due to the limited intensity available at the beamline, it has not been possible to record a time spectrum at the nuclear Bragg peak.

III. DISCUSSION

The difference in spin-dependent neutron reflectivities R^+ and R^- in Fig 4 is due to the ferromagnetic nature of the film. The Bragg peak is due to the isotopic periodicity of the multilayer. Its presence shows that no significant interdiffusion took place in the synthetic isotopically periodic multilayer prepared by using the MBE technique. The fact that the R^+ and R^- Bragg peaks in Fig. 4 appear almost exactly with the same intensity, shows that the SR was purely nuclear diffracted by the isotope periodicity of the multilayer. The slight deviation in the Q values of the Bragg peak measured with neutrons and photons is due to the difference in the critical angles of the total reflection as well as to the fact that with neutrons the whole area while with SR only a part of the somewhat inhomogeneous sample was measured.

The continuous curve on Fig. 5(b) corresponds to $D(\Theta) = \int_{t_1}^{t_2} R_t(t,\Theta)\,dt$. $R_t(t,\Theta)$ is calculated using an optical model[4] and with the provision that there was no preferred inplane direction of the magnetization within the film. For the calculation the layer parameters determined from neutron reflectivity fit was used. A universal roughness parameter was found from the fit to be $R_q = 1.2$ nm in accordance with the neutron data. The width of the Bragg peak also fairly accords with the expectations.

IV. CONCLUSION

We reported on the observation of a pure nuclear reflection of synchrotron radiation from a synthetic isotopically periodic multilayer prepared by MBE. This technique has proved to be suitable for fabricating synthetic isotopically periodic multilayers with no sign of layer interdiffusion. This is probably due to the fact that the target temperature is better controlled in MBE than in sputtering or conventional vacuum evaporation chambers. Using MBE for the preparation of synthetic isotopically periodic multilayers the crystalline and magnetic structure of the α phase of iron is maintained. The Bragg peak was strongly attenuated due to the roughness effects.

The main purpose of the study described here was to demonstrate the capabilities of MBE in fabricating narrow band monochromators rather than to build an operating device. For the latter purpose isotopically periodic but electronically homogeneous paramagnetic multilayers of broad resonance lines are, admittedly, better suited. A pure ferromagnetic α-iron multilayer has, however, the advantages that the experiment can be well compared with theory, the hyperfine interaction in the film being well defined. In contrast to a pure nuclear reflection of antiferromagnetic origin[8,9] that can be switched in a high external magnetic field the pure nuclear peak resulting from isotopic periodicity is not sensitive to external fields. Further, in low external fields the alignment of the sublayer magnetizations of an antiferromagnetic multilayer can be quite complicated,[9] a feature not expected for soft ferromagnetic materials like α-iron.

In conclusion, the present study is a contribution to developing efficient μeV monochromators for nuclear resonant scattering experiments at synchrotrons.

ACKNOWLEDGMENTS

This work was partly supported by the PHARE ACCORD Program under Contract No. H-9112-0522 and by the Hungarian Scientific Research Fund (OTKA) under Contract Nos. 1809, T016667, and F022150. The neutron reflectometry measurement at JINR was partly supported by the Dubna Fund of the Hungarian Government and by the INTAS Grant No. 93/3617. The authors also thankful for the partial support of the Deutsche Forschungsgemeinschaft, the Deutscher Akademischer Austauschdienst (DAAD), the Hungarian Academy of Sciences and the Polish Academy of Sciences in frames of bilateral projects. The Auger electron spectroscopy, scanning tunelling microscopy and profilometry measurements were part of Grant No. ERBCIPACT922051 of the Commission of the European Communities. Helpful discussions with Dr. A.I. Chumakov are gratefully acknowledged.

[1] D. L. Nagy and V. V. Pasyuk, Hyperfine Interact. **71**, 1349 (1992).
[2] L. Deák, L. Bottyán, and D. L. Nagy, in *Condensed Matter Studies by Nuclear Methods*, Proc. XVIII, Zakopane School of Physics, Zakopane, 1993, edited by E. A. Gorlich and K. Tomala (Institute of Nuclear Physics, Kraków, 1993), p. 269.
[3] L. Deák, L. Bottyán, and D. L. Nagy, Hyperfine Interact. **92**, 1083 (1994).
[4] L. Deák, L. Bottyán, D. L. Nagy, and H. Spiering, Phys. Rev. B **53**, 6158 (1996).
[5] A. Q. R. Baron, J. Arthur, S. L. Ruby, A. I. Chumakov, G. V. Smimov, and G. S. Brown, Phys. Rev. B **50**, 10354 (1994).
[6] J. P. Hannon, N. V. Hung, G. T. Trammell, E. Gerdau, M. Mueller, R. Rüffer, and H. Winkler, Phys. Rev. B **32**, 5068 (1984).
[7] J. P. Hannon, G. T. Trammell, M. Mueller, E. Gerdau, R. Rüffer, and H. Winkler, Phys. Rev. B **32**, 6363 (1985).
[8] T. S. Toellner, W. Sturhahn, R. Röhlsberger, E. E. Alp, C. H. Sowers, and E. E. Fullerton, Phys. Rev. Lett. **74**, 3475 (1995).
[9] L. Bottyán, J. Dekoster, L. Deák, A. Q. R. Baron, S. Degroote, R. Moons, D. L. Nagy, and G. Langouche, Hyperfine Interact. **113**, 295 (1998).
[10] G. T. Trammell, J. P. Hannon, S. L. Ruby, P. Flinn, R. L. Mössbauer, and F. Parak, AIP Conf. Proc. **38**, 46 (1977).
[11] V. A. Kabannik, *Version of a Nuclear Resonance Filter for Mössbauer Diffraction with Synchrotron Radiation* (in Russian), preprint (Institute of Nuclear Physics, 1989).
[12] S. Kikuta, X. Zhang, Y. Yoda, K. Izumi, and T. Ishikawa, Rev. Sci. Instrum. **60**, 2126 (1989).
[13] A. I. Chumakov and G. V. Smirnov, Pis'ma Zh. Eksp. Teor. Fiz. **53**, 258 (1991) [JETP Lett. **54**, 271 (1991)].
[14] A. I. Chumakov (private communication).
[15] A. I. Chumakov, G. V. Smirnov, S. S. Andreev, N. N. Salashchenko, and S. I. Shinkarev, Pis'ma Zh. Eksp. Teor. Fiz. **54**, 220 (1991) [JETP Lett. **55**, 509 (1992)].
[16] A. I. Chumakov, G. V. Smirnov, S. S. Andreev, N. N. Salashchenko, and S. I. Shinkarev, Pis'ma Zh. Eksp. Teor. Fiz. **55**, 495 (1992) [JETP Lett. **54**, 216 (1991)].
[17] A. I. Chumakov, G. V. Smirnov, A. Q. R. Baron, J. Arthur, D. E. Brown, S. L. Ruby, G. S. Brown, and N. N. Salashchenko, Phys. Rev. Lett. **71**, 2489 (1993).
[18] R. Röhlsberger, E. Witthoff, E. Lüken, and E. Gerdau, J. Appl. Phys. **74**, 1933 (1993).
[19] M. Born, E. Wolf, *Principles of Optics* (Pergamon P, Oxford, 1970), p. 51.
[20] F. Pászti, A. Manuaba, C. Hajdu, A. A. Melo, and M. F. da Silva, Nucl. Instrum. Methods Phys. Res. B **47**, 187 (1990).
[21] E. Kótai, Nucl. Instrum. Methods Phys. Res. B **85**, 588 (1994).
[22] J. Penfold and R. K. Thomas, J. Phys.: Condens. Matter **2**, 1369 (1990).
[23] D. A. Korneev, V. V. Pasyuk, A. V. Petrenko, and E. B. Dokukin in *Surface X-ray and Neutron Scattering*, edited by H. Zabel and I. K. Robinson (Springer, Berlin, 1992), p. 213.